Electronic Supplementary Material (ESI) for Chemical Communications.

Stable Pseudo[3]rotaxanes with Strong Positive Binding Cooperativity Based on Shape-Persistent Aromatic Oligoamide Macrocycles

Thomas A. Sobiech,‡[a] Yulong Zhong,‡[a] Laura S. Sánchez B.,[b] Brice Kauffmann,[c] Jillian K. McGrath,[a] Christina Scalzo,[a] Daniel P. Miller,[b] Ivan Huc,[d] Eva Zurek,[a] Yann Ferrand[c] and Bing Gong*[a]

[a.]Department of Chemistry, University at Buffalo, the State University of New York, Buffalo, New York 14260, United States.
[b.]Department of Chemistry 151 Hofstra University 106F Berliner Hall Hempstead, NY 11549, United States.
[c.]Institut Européen de Chimie et Biologie, UMS3011/US001 CNRS, Inserm, Université de Bordeaux, 2 rue Robert Escarpit, F-33600 Pessac, France .
[d.]Department Pharmazie, Ludwig-Maximilians-Universität München, Butenandtstraße 5-13, D-81377 Munich, Germany
‡These authors contributed equally to this work.

Supporting Information

I. Supporting Figures

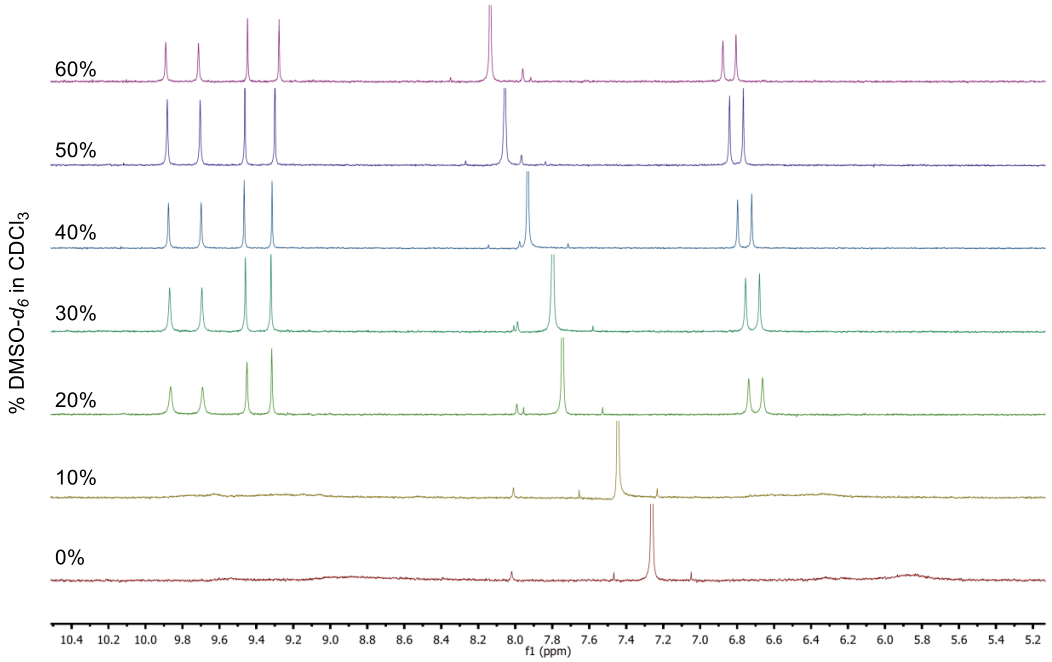

Figure S1. Partial ^{1}H NMR (500 MHz, 25°C) spectra of **2a** (1 mM) in $CDCl_3$ containing various volume percent of DMSO-d_6.

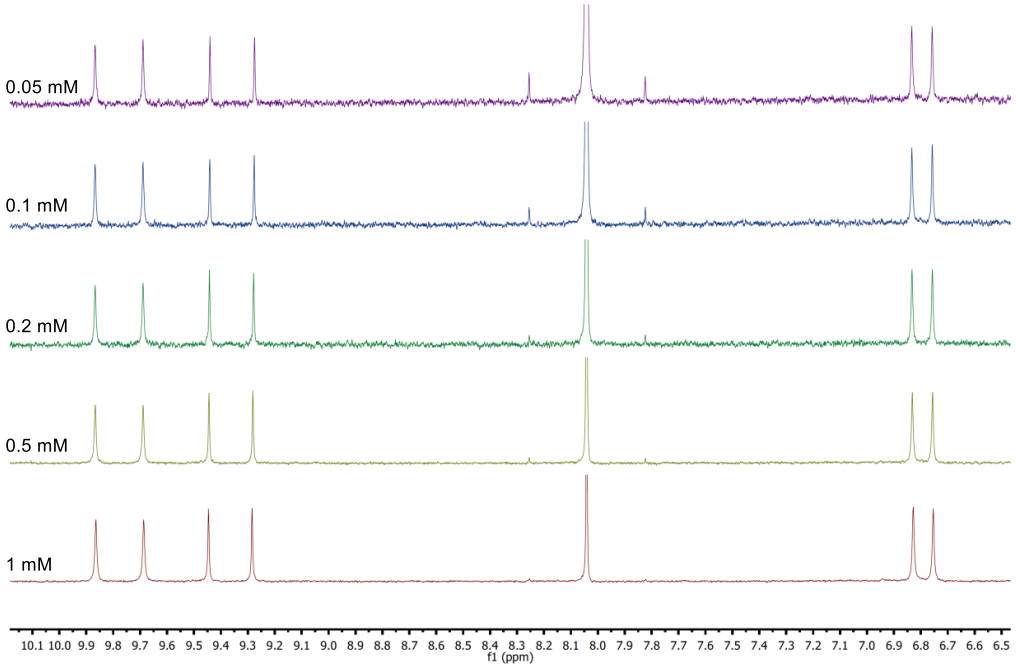

Figure S2. Partial ^{1}H NMR (500 MHz, 25°C) spectra of **2a** from 1 – 0.05 mM in DMSO-d_6/$CDCl_3$ (1:1, v/v).

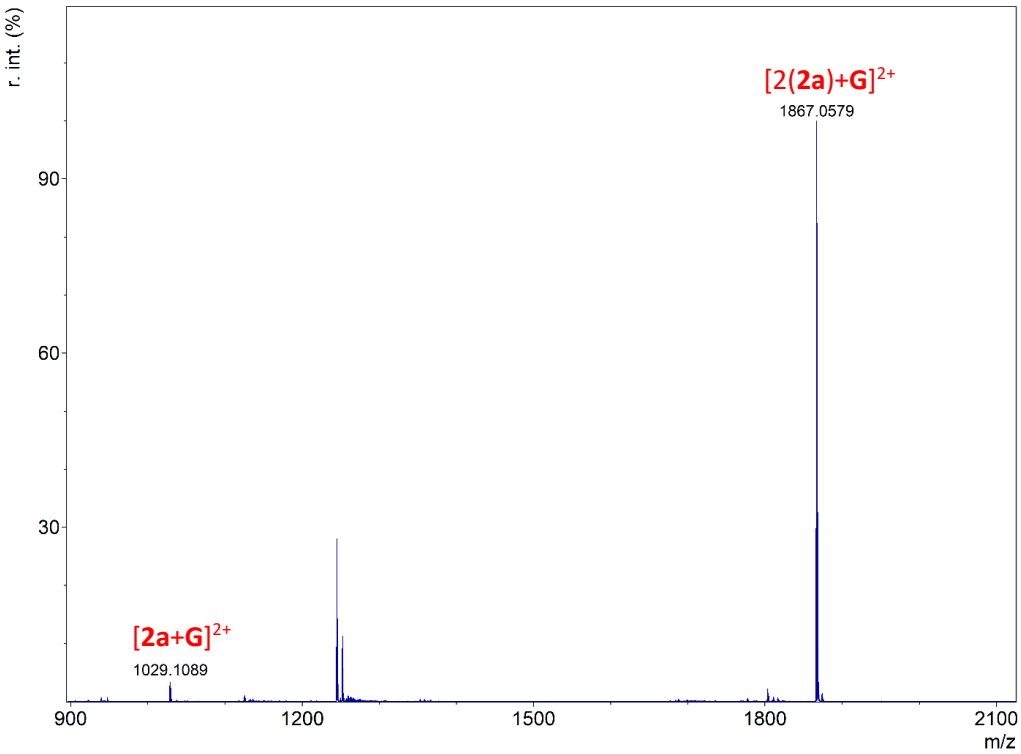

Figure S3a. ESI-QTOF mass spectrum of **2a** with **G**.

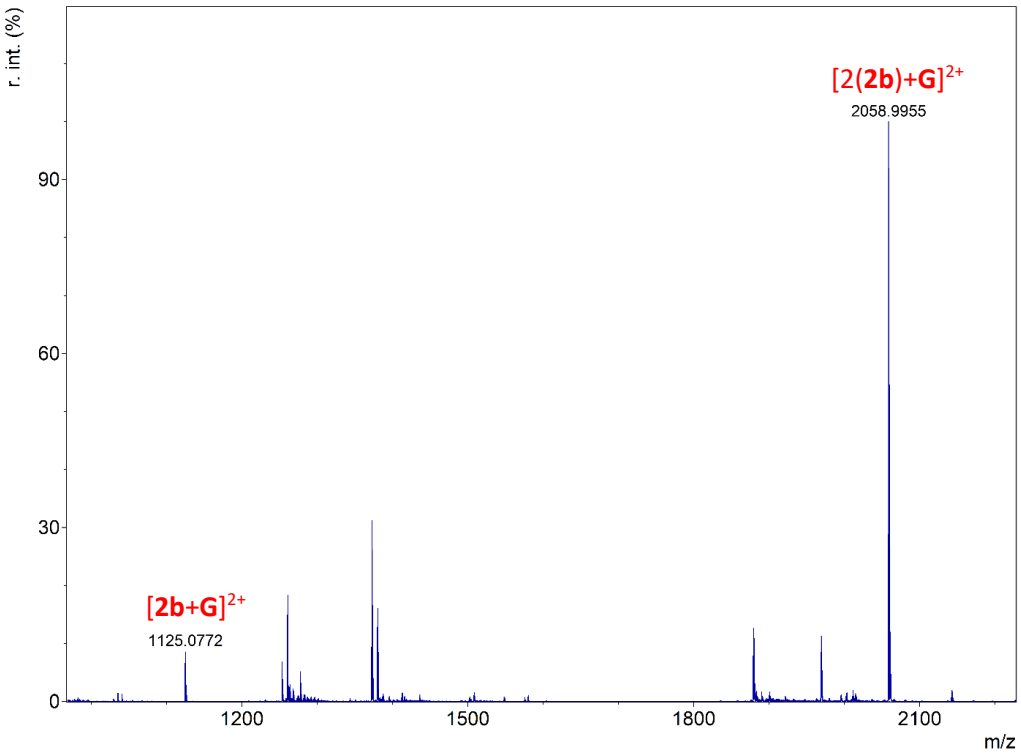

Figure S3b. ESI-QTOF mass spectrum of **2b** with **G**.

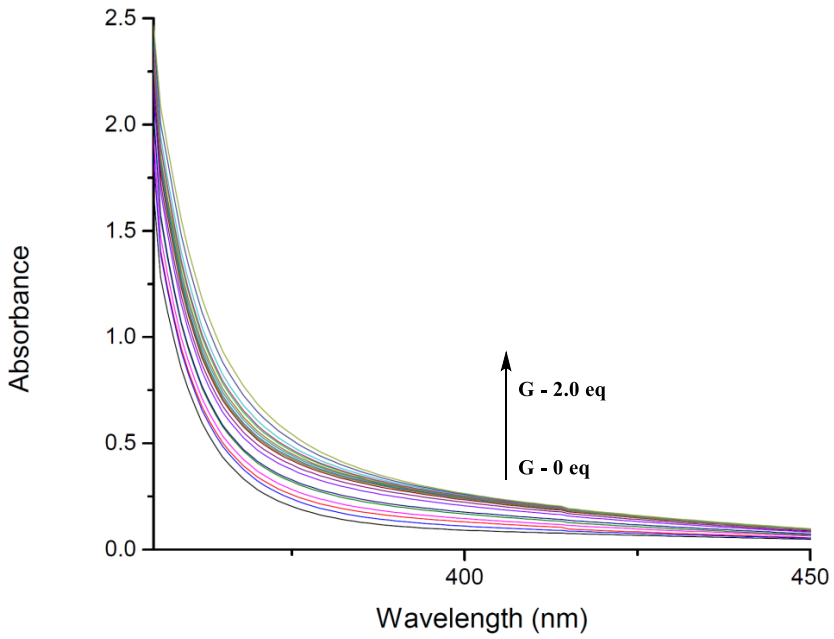

Figure S4a. Stacked UV-Vis spectra of **2a** (1 mM) titrated with Oct-PQ in DMSO/$CHCl_3$ (1:1, v/v) from 0 equiv. to 2 equiv. at 25°C. The measurements were performed with 1 mM of **2a** in order to monitor the change in the new minor absorbance band emerging from complex formation in the 400 – 450 nm region.

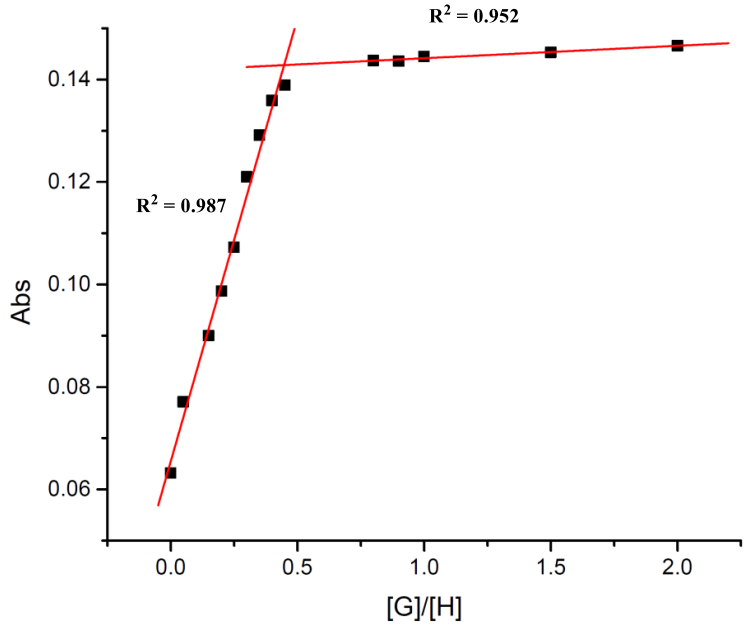

Figure S4b. UV-Vis mole ratio plot for the complexation of **2a** and **G** in DMSO/$CHCl_3$ (1:1, v/v) at 25°C indicating a 2:1 stoichiometry from the change in abs at 430 nm.

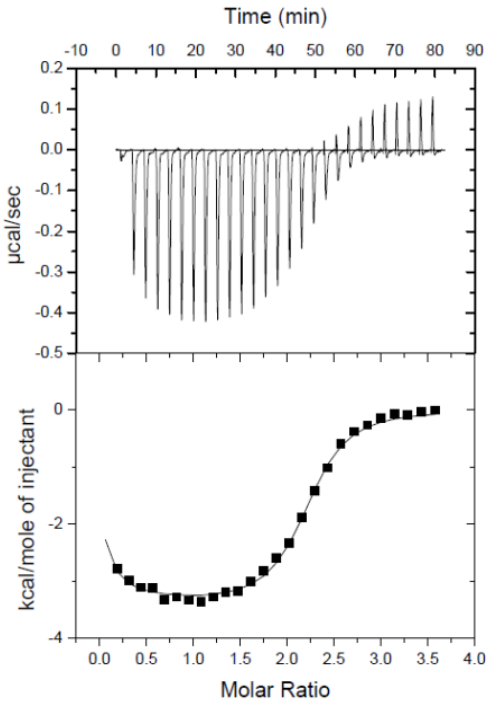

Figure S5a. ITC titration plot for **2a** (450 µM) titrated into cell containing **G** (25 µM) in DMSO/$CHCl_3$ (1:1, v/v) at 25°C. Data was fit to sequential binding model with number of sites equal to two.

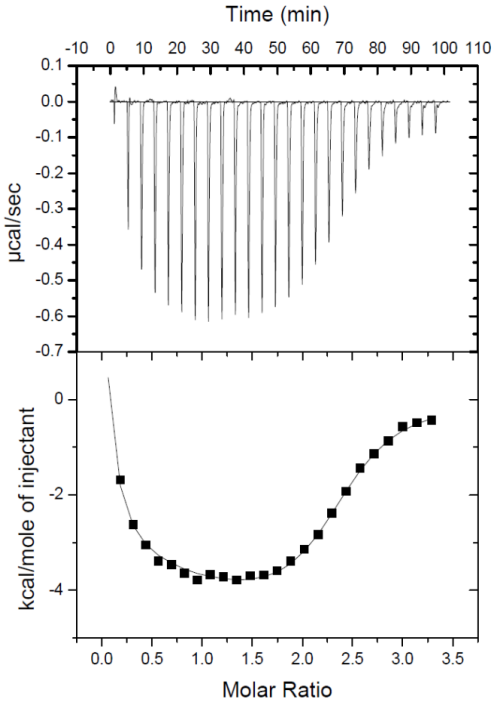

Figure S5b. ITC titration plot for **2b** (450 µM) titrated into cell containing **G** (25 µM) in DMSO/$CHCl_3$ (1:1, v/v) at 25°C. Data was fit to sequential binding model with number of sites equal to two.

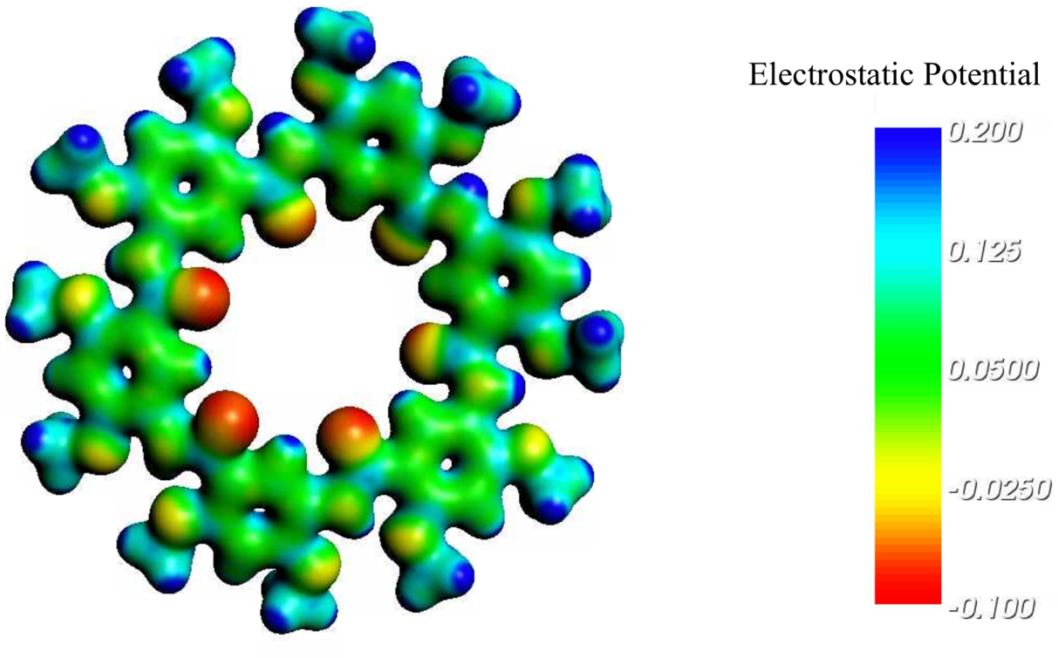

Figure S6a: The electrostatic potential (ESP) of the macrocycle **2** (Isovalue = 0.03 a.u.). The ESP scale bar displays the attraction with positive charges (red) and repulsion with positive charges (blue). The R side chains of **2** are replaced with methyl groups.

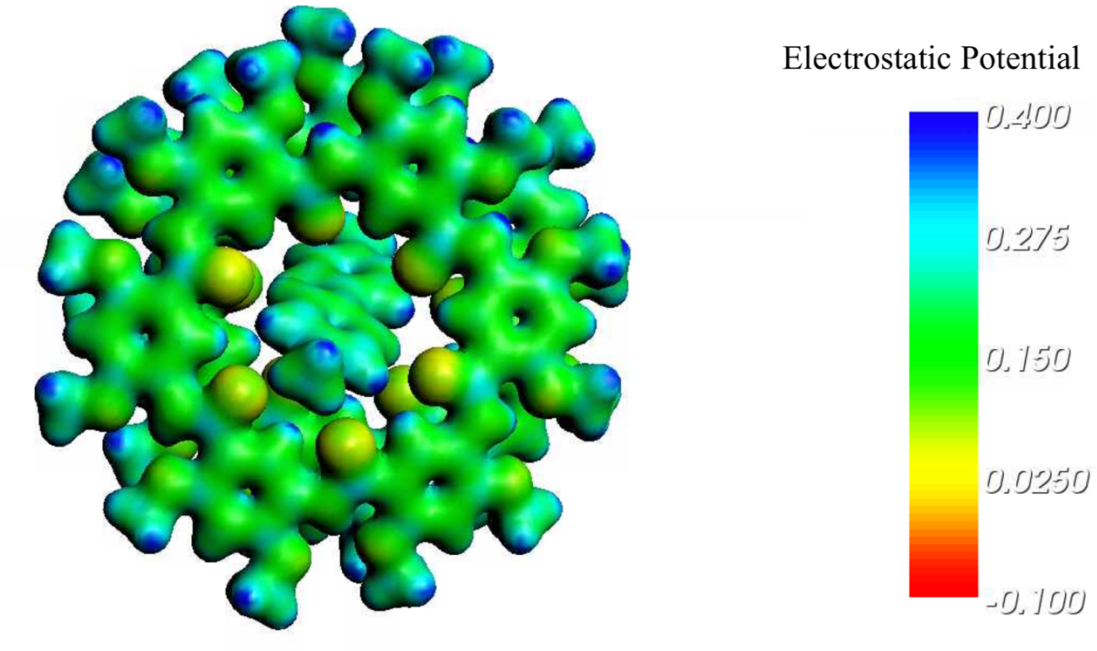

Figure S6b: The electrostatic potential (ESP) of the 2:1 complex $\mathbf{2_2 \bullet G}$ (Isovalue = 0.03 a.u.). The ESP scale bar displays the attraction with positive charges (red) and repulsion with positive charges (blue). The octyl end groups of guest **G** and the R side chains of **2** are replaced with methyl groups.

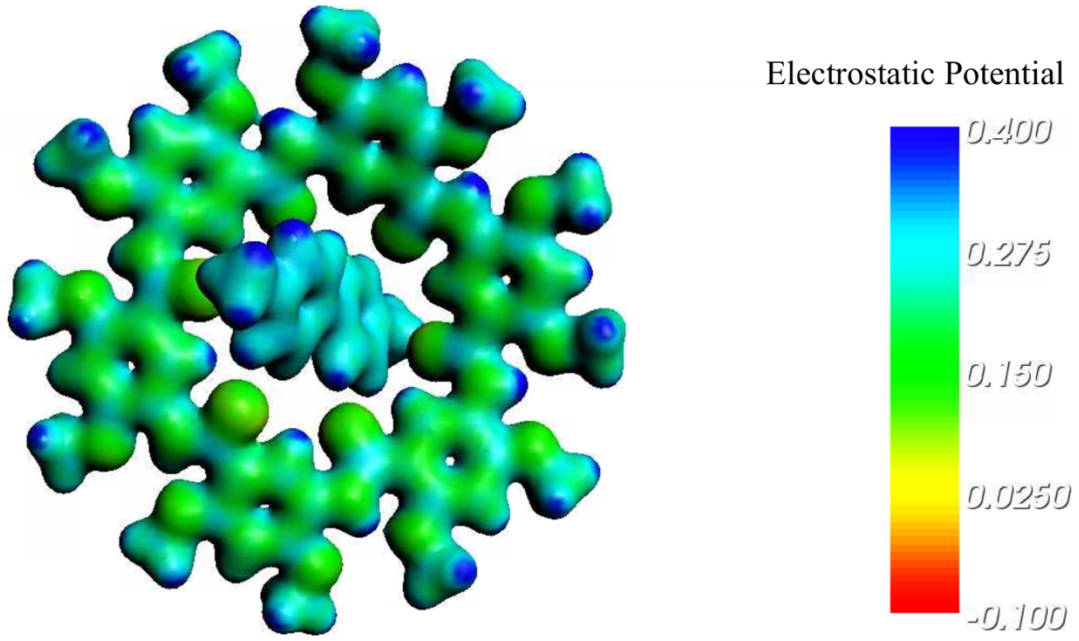

Figure S6c: The electrostatic potential (ESP) of the 1:1 complex **2•G** (Isovalue = 0.03 a.u.). The ESP scale bar displays the attraction with positive charges (red) and repulsion with positive charges (blue). The octyl end groups of guest **G** and the R side chains of **2** are replaced with methyl groups.

The stronger binding of the 2:1 complex versus the 1:1 complex is supported by a cooperative influence displayed in the electrostatic potentials. The macrocycle **2** has a strong propensity to attract positive charges within the pore at the oxygen atoms, which is shown with the red coloring. The positively charged paraquat guest is attracted to the negatively charged pore of the macrocycle **2**. The 1:1 complex shows the oxygen become more attracted to negative charges than positive charges given the green coloring in the ESP. Such a change in charge attraction does not support strong binding to a positively charged species. The 2:1 complex shows the oxygen retain its attraction to positive charges with yellow coloring in the ESP. The guest **G** in the 1:1 complex retains a strong repulsion to positive charges while the guest **G** in the 2:1 complex induces a lower repulsion to positive charges. This delicate balance in the 2:1 complex with the oxygen retaining positive charge attraction and the guest **G** being less repulsive to other atoms in the host supports our cooperative and strong 2:1 binding.

II. General Remarks

Chemicals were purchased from commercial sources and used as received. Unless otherwise specified, all solvents were removed with a rotary evaporator. Silica gel for analytical thin layer chromatography (TLC) and column chromatography (mesh 230~400) were purchased from Sorbent Technologies Inc. ^{1}H NMR spectra were recorded at 300 MHz, 400 MHz and 500 MHz and ^{13}C NMR spectra were measured at 75 MHz, 101 MHz, 126 MHz at ambient temperature using $CDCl_3$ or DMSO-d_6 as solvent (Cambridge Isotope Laboratories, Inc.) on Varian Mercury-300, Varian Inova-400 and Varian Inova-500. Chemical shifts are reported in parts per million (ppm) downfield from TMS (tetramethylsilane). Coupling constant in ^{1}H NMR are expressed in Hertz (Hz). The solubility of **2a** improved upon the addition of tetraethylammonium chloride (TEA-Cl), the ^{13}C NMR spectrum of **2a** was obtained in the presence of 5 equiv. of TEA-Cl. Regular and high-resolution mass spectra were recorded on a Thermo-LTQ XL LC/MS and 6530 Q-TOF LC/MS. UV-Vis spectroscopy experiments were performed using a DU800 UV/Visible Spectrophotometer. ITC experiments were performed using a MicroCal VP-ITC. ITC experiments were conducted by adding ~1.5 mL of solution containing **G** to the ITC sample cell followed by the addition of **2a** or **2b** from the syringe in 10 μL aliquots. Heats of dilution were obtained by titrating either **2a** or **2b** into the ITC sample cell in the absence of **G**. These heats were found to be negligible when compared to the binding interaction heats. ITC data was processed and fit using the origin program (MicroCal).

III. Synthesis and Characterization

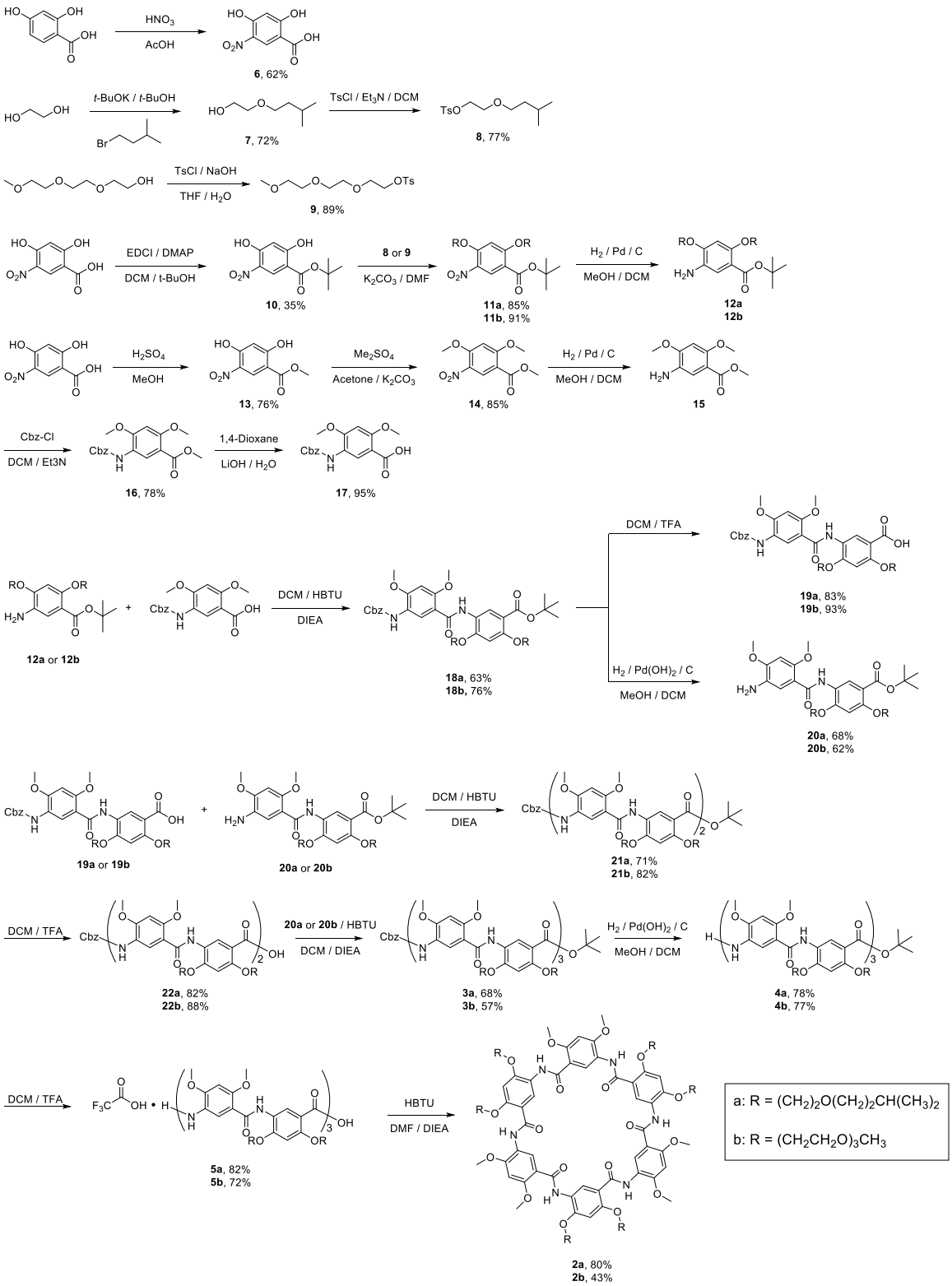

Scheme S1. Synthetic route for macrocycles **2a** and **2b**.

Compounds **6**, **7**, **8**, **9**, **10**, **11a**, **12a**, **13**, **14**, **15**, **16**, **17**, **18a**, **19a**, **20a**, **21a**, **22a**, **3a** and **4a** were synthesized according to previously reported procedures.[1,2]

Compound 11b. Compound **10** (10.0 g, 39.2 mmol) was dissolved in DMF (200 mL), to which K_2CO_3 (32.5 g, 0.235 mol) and compound **9** (37.4 g, 0.118 mol) were added. The mixture was heated at 80°C for overnight. After adding water (600 mL), the reaction mixture was stirred for another 30 minutes, and then attracted with ethyl acetate (3 x 100 mL), washed with water (3 x 500 mL). The organic phase was combined and concentrated. The residue was then purified with flash column chromatography (DCM:MeOH = 20:1) to give **11b** as a yellow oil (19.5 g, 91%). ^{1}H NMR (300 MHz, $CDCl_3$) δ 8.10 (s, 1H), 6.45 (s, 1H), 4.09 – 3.93 (m, 4H), 3.61 (s, 4H), 3.48 – 3.38 (m, 4H), 3.31 (m, 8H), 3.21 (m, 4H), 3.03 (d, *J* = 2.6 Hz, 6H), 1.26 (m, 9H). ^{13}C NMR (75 MHz, $CDCl_3$) δ 163.0, 156.7, 131.6, 130.2, 113.9, 99.2, 81.3, 77.9, 77.5, 77.1, 71.5, 70.7, 70.5, 70.2, 70.1, 70.0, 69.7, 69.1, 69.0, 68.9, 58.5, 58.5, 53.5, 27.9. MS (ESI-TOF) m/z: $[M + Na]^+$ Calcd for $C_{25}H_{41}NO_{12}Na$ 570.3, found 570.6.

Compound 12b. Compound **11b** (10.0 g, 18.3 mmol) was dissolved in DCM (50 mL) and methanol (50 mL), to which palladium on carbon (1 g, 10%wt) was added. The mixture was reacted under hydrogen gas (40 psi) until the starting materials disappeared. After removing the catalyst by filtration, the solution was concentrated under reduced pressure to remove the solvents. The crude product was directly used for the next step without further purification.

General Synthetic Procedure for Group Deprotection and Coupling.

***tert*-Butyl ester deprotection**

To a solution of TFA (5.0 mL) in CH_2Cl_2 (20.0 mL) was added the corresponding *tert*-butyl protected compound. The solution was stirred for at least 1 hour at room temperature until the starting material disappeared as monitored by TLC. Upon the completion of reaction, all solvents were removed under vacuum to give the product as pure.

Removal of the CBZ group

The CBZ-protected compound was dissolved in CH_2Cl_2 (50.0 mL) and MeOH (20.0 mL), to which $Pd(OH)_2$ (20%wt, 50% water) was added. The mixture was reacted under hydrogen gas (40 psi) until the starting materials disappeared. After removing the catalyst by filtration, the filtrate was concentrated under reduced pressure to give the product as pure.

Coupling of acid and amine

To the solution of the corresponding acid (1 equiv.) and amine (1 equiv.) in dry CH_2Cl_2, HBTU (1.1 equiv.) and DIEA (3.0 equiv.) were added. The mixture was stirred overnight at room temperature. Removal solvent under vacuum gave rise to the crude product which was then subject to silica gel chromatography ($CHCl_3$:MeOH = 40:1 to 10:1). The pure product was obtained as a solid.

Compound 18b. White solid (76%). ^{1}H NMR (400 MHz, $CDCl_3$) δ 10.08 (s, 1H), 8.98 (s, 1H), 8.70 (s, 1H), 7.42 – 7.36 (m, 2H), 7.36 – 7.22 (m, 3H), 6.87 (s, 1H), 6.36 (s, 1H), 6.29 (s, 1H), 5.17 (s, 2H), 4.10 (t, *J* = 4.5 Hz, 2H), 4.06 (t, *J* = 5.1 Hz, 2H), 3.92 (s, 3H), 3.83 (m, 4H), 3.78 (s, 3H), 3.71 (m, 2H), 3.66 – 3.56 (m, 8H), 3.56 – 3.46 (m, 4H), 3.46 – 3.38 (m, 2H), 3.33 (s, 3H), 3.28 (s, 3H), 1.56 (s, 9H). ^{13}C NMR (101 MHz, $CDCl_3$) δ 165.3, 162.2, 154.8, 150.8, 136.3, 128.5, 128.4, 128.2, 122.8, 122.5, 120.7, 114.9, 114.1, 98.7, 94.8,

80.4, 77.4, 77.1, 76.8, 71.9, 71.8, 70.8, 70.6, 70.5, 70.4, 69.7, 69.5, 69.3, 68.1, 66.9, 59.0, 58.9, 56.4, 55.8, 28.3. MS (ESI-TOF) m/z: $[M + Na]^+$ Calcd for $C_{42}H_{58}N_2O_{15}Na$ 853.4, found 854.0.

Compound 19b. White solid (93%). ^1H NMR (400 MHz, $CDCl_3$) δ 10.15 (s, 1H), 9.06 (s, 1H), 8.60 (s, 1H), 7.41 – 7.21 (m, 5H), 6.97 (s, 1H), 6.46 (s, 1H), 6.37 (s, 1H), 5.14 (s, 2H), 4.23 (m, 2H), 4.19 (m, 2H), 3.95 (s, 3H), 3.91 (m, 2H), 3.82 (s, 3H), 3.76 (m, 2H), 3.65 (m, 6H), 3.61 – 3.56 (m, 4H), 3.54 (m, 2H), 3.48 (m, 2H), 3.43 (m, 2H), 3.31 (s, 3H), 3.27 (s, 3H). ^{13}C NMR (101 MHz, $CDCl_3$) δ 165.7, 162.4, 154.6, 154.2, 152.9, 136.3, 128.5, 128.3, 128.2, 123.6, 123.5, 120.7, 113.2, 109.6, 97.5, 94.9, 77.4, 77.1, 76.8, 71.8, 70.5, 70.4, 69.4, 69.2, 68.8, 68.6, 66.8, 58.9, 56.4, 56.0, 54.8, 42.8, 18.6, 17.1, 12.5. MS (ESI-TOF) m/z: $[M + Na]^+$ Calcd for $C_{38}H_{50}N_2O_{15}Na$ 797.3, found 797.7.

Compound 20b. White solid (62%). ^1H NMR (300 MHz, $CDCl_3$) δ 10.23 (s, 1H), 8.92 (s, 1H), 7.59 (s, 1H), 6.44 (s, 1H), 6.32 (s, 1H), 4.14 (d, *J* = 5.2 Hz, 2H), 4.08 (d, *J* = 5.3 Hz, 2H), 3.90 (d, *J* = 2.0 Hz, 3H), 3.87 – 3.74 (m, 7H), 3.69 (d, *J* = 6.3 Hz, 2H), 3.66 – 3.55 (m, 8H), 3.53 (m, 2H), 3.51 – 3.45 (m, 2H), 3.42 (m, 2H), 3.30 (s, 3H), 3.27 (s, 3H), 1.53 (s, 9H). ^{13}C NMR (75 MHz, $CDCl_3$) δ 165.3, 162.8, 154.9, 151.6, 151.0, 150.9, 129.3, 122.9, 122.4, 117.8, 114.9, 114.0, 98.9, 95.8, 80.4, 77.6, 77.2, 76.8, 71.9, 71.8, 70.8, 70.6, 70.5, 70.4, 69.8, 69.5, 69.3, 68.2, 59.0, 58.9, 56.8, 55.6, 28.3. MS (ESI-TOF) m/z: $[M + Na]^+$ Calcd for $C_{34}H_{52}N_2O_{13}Na$ 719.3, found 720.0.

Compound 21b. White solid (82%). ^1H NMR (300 MHz, $CDCl_3$) δ 10.12 (s, 1H), 10.03 (s, 1H), 9.72 (s, 1H), 9.23 (s, 1H), 9.08 (s, 2H), 8.69 (s, 1H), 7.48 – 7.40 (m, 3H), 7.40 – 7.32 (m, 2H), 6.92 (s, 1H), 6.45 (s, 1H), 6.38 (s, 1H), 6.32 (m, 2H), 5.22 (s, 2H), 4.13 (m, 8H), 3.99 (s, 6H), 3.95 – 3.81 (m, 11H), 3.80 – 3.73 (m, 5H), 3.72 – 3.52 (m, 20H), 3.51 – 3.38 (m, 10H), 3.36 (m, 3H), 3.31 (m, 3H), 3.27 (m, 6H), 1.66 – 1.58 (s, 9H). ^{13}C NMR (75 MHz, $CDCl_3$) δ 165.2, 162.6, 162.5, 162.0, 154.9, 154.5, 153.1, 153.0, 151.3, 151.0, 136.4, 128.6, 128.5, 128.3, 125.0, 123.8, 123.0, 122.7, 121.9, 120.5, 114.8, 114.3, 114.0, 113.7, 98.9, 97.0, 94.8, 80.5, 77.5, 77.0, 76.6, 71.9, 71.8, 70.8, 70.6, 70.5, 70.4, 70.3, 69.8, 69.6, 69.4, 69.2, 68.9, 68.3, 68.2, 66.9, 59.0, 58.9, 56.5, 56.4, 56.0, 55.8, 28.4. MS (ESI-TOF) m/z: $[M + H]^+$ Calcd for $C_{72}H_{101}N_4O_{27}$ 1453.7, found 1453.9.

Compound 22b. White solid (88%). ^1H NMR (300 MHz, $CDCl_3$) δ 10.09 (s, 2H), 9.72 (s, 1H), 9.23 (s, 1H), 9.17 (s, 1H), 9.03 (s, 1H), 8.67 (s, 1H), 7.38 (m, 5H), 6.97 (s, 1H), 6.39 (s, 1H), 6.36 – 6.25 (s, 2H), 6.23 (s, 1H), 5.20 (s, 2H), 4.28 (s, 2H), 4.13 (s, 6H), 4.01 (m, 6H), 3.94 (s, 4H), 3.85 (s, 6H), 3.79 – 3.66 (m, 10H), 3.66 – 3.58 (m, 10H), 3.58 – 3.52 (m, 4H), 3.52 – 3.45 (m, 6H), 3.41 (m, 6H), 3.32 (s, 3H), 3.25 (s, 9H). ^{13}C NMR (75 MHz, $CDCl_3$) δ 165.6, 162.4, 162.1, 161.9, 154.5, 153.7, 153.0, 152.7, 151.3, 136.3, 128.6, 128.4, 128.3, 123.9, 122.7, 121.4, 120.4, 113.7, 112.9, 109.5, 77.6, 77.2, 76.7, 71.8, 71.7, 70.5, 70.4, 70.3, 70.2, 68.6, 66.9, 58.9, 58.8, 56.5, 56.2, 55.9. MS (ESI-TOF) m/z: $[M + Na]^+$ Calcd for $C_{68}H_{92}N_4O_{27}Na$ 1419.6, found 1420.2.

Compound 3b. White solid (57%). ^1H NMR (400 MHz, $CDCl_3$) δ 10.17 (s, 1H), 10.06 (m, 2H), 9.76 (m, 2H), 9.22 (m, 2H), 9.06 (m, 2H), 8.98 (s, 1H), 8.71 (s, 1H), 7.43 (m, 2H), 7.37 (m, 2H), 7.31 (m, 1H), 6.95 (s, 1H), 6.55 – 6.37 (m, 6H), 5.21 (s, 2H), 4.29 – 4.17 (m, 10H), 4.14 (m, 2H), 4.09 – 4.00 (m, 9H), 3.95 (m, 10H), 3.88 (m, 6H), 3.83 (s, 3H), 3.79 – 3.68 (m, 8H), 3.65 (m, 14H), 3.61 – 3.53 (m, 10H), 3.53 – 3.46 (m, 10H), 3.46 – 3.43 (m, 4H), 3.41 (m, 4H), 3.37 (s, 3H), 3.31 (s, 3H), 3.27 (m, 12H), 1.60 (s, 9H). ^{13}C NMR (101 MHz, $CDCl_3$) δ 165.2, 162.8, 162.6, 162.4, 162.1, 155.0, 154.8, 154.7, 153.6, 153.3, 153.2, 151.7, 151.6, 151.0, 136.4, 128.6, 128.4, 128.2, 123.9, 123.1, 123.0, 122.8, 122.0, 121.6, 120.7, 115.1, 114.6, 114.2, 113.9, 113.8, 99.3, 97.6, 97.5, 95.2, 95.0, 80.5, 77.4, 77.1, 76.8, 71.9, 71.8, 70.8, 70.6, 70.5, 70.4, 70.3,

69.8, 69.5, 69.4, 69.3, 69.1, 68.6, 68.5, 68.3, 66.9, 59.0, 58.8, 56.7, 56.5, 56.4, 56.1, 55.9, 29.7, 28.4. MS (ESI-TOF) m/z: $[M + H]^+$ Calcd for $C_{102}H_{143}N_6O_{39}$ 2076.9, found 2077.5.

Compound 4a. Grey solid (78%). ^{1}H NMR (400 MHz, DMSO-d_6 / $CDCl_3$ (3/7, v/v)) δ 10.31 (s, 2H), 10.28 (s, 1H), 10.14 (s, 1H), 10.11 (s, 1H), 9.33 (s, 1H), 9.26 (s, 1H), 9.19 (s, 1H), 9.09 (s, 1H), 8.95 (s, 1H), 8.05 (s, 1H), 6.84 (s, 1H), 6.82 (s, 1H), 6.71 (s, 3H), 6.68 (s, 1H), 4.42 (s, 4H), 4.37 – 4.34 (m, 6H), 4.30 (s, 4H), 4.15 (s, 3H), 4.13 (s, 3H), 4.11 (s, 3H), 4.07 (s, 3H), 4.06 (s, 3H), 4.02 (s, 3H), 3.92 – 3.86 (m, 12H), 3.81 – 3.74 (m, 2H), 3.61 – 3.46 (m, 14H), 1.78 – 1.62 (m, 4H), 1.55 (s, 9H), 1.51 – 1.41 (m, 10H), 1.37 – 1.34 (m, 4H), 0.91 – 0.78 (m, 36H). ^{13}C NMR (75 MHz, DMSO-d_6 / $CDCl_3$ (3/7, v/v)) δ 162.5, 162.2, 161.1, 158.0, 155.9, 154.7, 153.5, 153.0, 151.4, 151.1, 124.5, 123.1, 122.6, 122.2, 115.1, 114.2, 113.5, 99.1, 98.4, 96.7, 95.6, 69.6, 68.8, 56.7, 56.4, 38.4, 28.3, 24.9, 22.7. MS (ESI-TOF) m/z: $[M + H]^+$ Calcd for $C_{94}H_{137}N_6O_{25}$ 1751.0, found 1751.6.

Compound 4b. Grey solid (77%). ^{1}H NMR (400 MHz, DMSO-d_6/$CDCl_3$ (3/7 v/v)) δ 10.23 (s, 2H), 10.09 (s, 1H), 10.03 (m, 2H), 9.23 (s, 1H), 9.13 (s, 2H), 9.02 (s, 1H), 8.83 (s, 1H), 8.20 (s, 1H), 6.77 (s, 1H), 6.73 (s, 1H), 6.69 (s, 1H), 6.65 (s, 2H), 6.59 (s, 1H), 4.35 (m, 4H), 4.29 (m, 4H), 4.25 – 4.20 (m, 2H), 4.06 (m, 11H), 4.01 – 3.92 (m, 9H), 3.87 (m, 10H), 3.74 (m, 2H), 3.57 (m, 20H), 3.47 (m, 12H), 3.39 (m, 12H), 3.34 – 3.27 (m, 4H), 3.25 – 3.14 (m, 18H), 1.45 (s, 9H). ^{13}C NMR (101 MHz, DMSO-d_6/$CDCl_3$ (3/7 v/v)) δ 165.4, 162.4, 162.2, 161.0, 158.6, 156.2, 154.9, 154.7, 153.5, 153.4, 153.2, 152.9, 151.4, 151.1, 123.1, 122.5, 122.2, 122.1, 114.5, 114.4, 114.2, 113.7, 113.5, 110.0, 99.1, 98.4, 95.6, 80.3, 78.9, 78.8, 78.6, 78.3, 71.8, 71.7, 70.6, 70.5, 70.4, 70.3, 70.2, 69.7, 69.6, 69.3, 69.2, 68.7, 68.5, 58.7, 58.6, 57.0, 56.8, 56.4, 40.7, 40.5, 40.3, 40.1, 39.9, 39.7, 39.5, 36.4, 31.3, 28.3, 18.5. MS (ESI-TOF) m/z: $[M + H]^+$ Calcd for $C_{94}H_{137}N_6O_{37}$ 1942.9, found 1943.3.

Compound 5a. Compound **4a** (1.0 g, 0.57 mmol) was dissolved in 20 mL DCM and 4 mL TFA was added. After the starting material disappeared, all solvents were removed by rotary evaporation to give compound **5a** as a dark brown solid (0.85 g, 82%). ^{1}H NMR (400 MHz, DMSO-d_6) δ 10.34 (s, 1H), 10.31 (s, 1H), 10.30 (s, 1H), 10.13 (s, 2H), 9.24 (s, 2H), 9.08 (s, 1H), 9.04 (s, 1H), 8.99 (s, 1H), 7.66 (s, 1H), 6.87 (s, 1H), 6.85 (s, 1H), 6.80 (s, 1H), 6.78 (s, 2H), 6.71 (s, 1H), 4.42 – 4.25 (m, 10H), 4.19 (s, 2H), 4.07 (s, 6H), 4.02 (s, 3H), 4.00 (s, 6H), 3.90 (s, 3H), 3.87 – 3.75 (m, 10H), 3.70 (t, J = 4.8 Hz, 2H), 3.58 – 3.37 (m, 12H), 1.66 – 1.56 (m, 4H), 1.51 – 1.44 (m, 2H), 1.41 – 1.33 (m, 8H), 1.26 – 1.20 (m, 4H), 0.84 (d, J = 6.6 Hz, 6H), 0.80 – 0.77 (m, 18H), 0.71 – 0.68 (m, 12H). ^{13}C NMR (101 MHz, DMSO-d_6) δ 166.7, 162.3, 155.3, 154.7, 153.4, 153.2, 153.1, 152.6, 151.7, 151.4, 123.9, 122.8, 122.5, 122.2, 121.8, 114.0, 113.7, 113.2, 113.1, 112.5, 99.7, 98.8, 97.3, 96.2, 69.8, 69.7, 69.5, 69.3, 68.9, 68.7, 57.2, 56.9, 56.7, 56.4, 38.4, 25.0, 22.8. MS (ESI-TOF) m/z: $[M + Na]^+$ Calcd for $C_{90}H_{128}N_6O_{25}Na$ 1715.9, found 1716.5.

Compound 5b. Compound **4b** (1.0 g, 0.51 mmol) was dissolved in 20 mL DCM and 4 mL TFA was added. After the starting material disappeared, all solvents were removed by rotary evaporation to give compound **5b** as a light brown solid (0.69 g, 72%). ^{1}H NMR (300 MHz, DMSO-d_6) δ 10.35 (s, 2H), 10.28 (s, 1H), 10.14 (s, 2H), 9.27 (m, 2H), 9.14 (s, 1H), 9.09 (s, 1H), 9.01 (s, 1H), 8.16 (s, 1H), 6.94 (s, 1H), 6.89 (s, 2H), 6.83 (m, 3H), 4.36 (m, 10H), 4.21 (m, 2H), 4.16 – 3.93 (m, 18H), 3.86 (m, 10H), 3.76 (m, 2H), 3.61 (m, 8H), 3.52 (m, 12H), 3.46 (m, 8H), 3.41 (m, 6H), 3.35 (m, 10H), 3.31 – 3.23 (m, 4H), 3.22 (s, 3H), 3.18 – 3.08 (m, 15H). ^{13}C NMR (75 MHz, DMSO-d_6) δ 166.9, 162.4, 162.3, 162.2, 161.2, 159.0, 158.5, 158.3, 156.3, 155.4, 154.8, 153.7, 153.5, 153.2, 153.1, 151.7, 151.6, 122.8, 122.3, 122.2, 122.1, 115.1, 113.7, 113.6, 113.0, 112.8, 112.4, 96.4, 71.7, 71.6, 70.5, 70.3, 70.2, 70.1, 70.0, 69.6, 69.4, 69.2, 69.0, 58.5, 58.4,

57.5, 57.2, 57.1, 56.8, 40.7, 40.5, 40.2, 39.9, 39.6, 39.3, 39.1. MS (ESI-TOF) m/z: $[M + H]^+$ Calcd for $C_{90}H_{129}N_6O_{37}$ 1885.8, found 1886.0.

Compound 2a. Compound **5a** (0.20 g, 0.11 mmol) was dissolved in 100 mL DMF followed by adding 77 µL DIEA and HATU (50.2 mg, 0.13 mmol). The reaction was stirred for 24 hours and then concentrated in vacuo. The residue was then first purified with flash column chromatography ($CHCl_3$:MeOH = 20:1) followed by washing with MeOH to give **2a** as a white solid (147 mg, 80%). ^{1}H NMR (500 MHz, DMSO-d_6 / $CDCl_3$ (1/1, v/v)) δ 9.86 (s, 3H), 9.68 (s, 3H), 9.43 (s, 3H), 9.27 (s, 3H), 6.84 (s, 3H), 6.76 (s, 3H), 4.44 – 4.40 (m, 6H), 4.37 (s, 6H), 4.13 (s, 9H), 4.06 (s, 9H), 3.93 (t, *J* = 4.9 Hz, 6H), 3.91 – 3.88 (m, 6H), 3.56 (t, *J* = 6.8 Hz, 6H), 3.53 (t, *J* = 6.7 Hz, 6H), 1.75 – 1.66 (m, 3H), 1.66 – 1.59 (m, 3H), 1.48 (q, *J* = 6.8 Hz, 6H), 1.37 (q, *J* = 6.8 Hz, 6H), 0.88 (d, *J* = 6.7 Hz, 18H), 0.80 (d, *J* = 6.6 Hz, 18H). ^{13}C NMR (101 MHz, $CDCl_3$, with 5 equiv. tetraethyl ammonium chloride) δ 163.5, 163.2, 154.6, 153.4, 151.9, 126.7, 125.4, 122.7, 121.8, 114.5, 113.8, 97.4, 94.9, 69.9, 69.2, 69.0, 68.8, 68.4, 56.4, 56.2, 52.7, 52.1, 38.4, 25.1, 25.0, 22.6, 22.5, 7.8, 7.4. HRMS (ESI-QTOF) m/z: $[2M + H + Na]^{2+}$ Calcd for $C_{180}H_{253}N_{12}O_{48}Na$ 1687.3823, found 1687.3755.

Compound 2b. Compound **5b** (0.10 g, 0.050 mmol) was dissolved in 50 mL DMF followed by adding 38 µL DIEA and HATU (24.6 mg, 0.065 mmol). The reaction was stirred for 24 hours and then concentrated in vacuo. The residue was then purified with flash column chromatography (DCM:MeOH = 10:1) to give **2b** as a light yellow solid (42.9 mg, 46%). ^{1}H NMR (500 MHz, DMSO-d_6/$CDCl_3$ (1/1 v/v)) δ 9.82 (s, 3H), 9.62 (s, 3H), 9.45 (s, 3H), 9.29 (s, 3H), 6.82 (s, 3H), 6.76 (s, 3H), 4.38 (t, J = 4.7 Hz, 6H), 4.33 (s, 6H), 4.08 (s, 9H), 4.02 (s, 9H), 3.93 (t, J = 5.0 Hz, 6H), 3.89 (m, 6H), 3.64 (m, 12H), 3.56 (m, 6H), 3.49 (m, 12H), 3.45 – 3.41 (m, 6H), 3.39 – 3.37 (m, 6H), 3.34 – 3.31 (m, 6H), 3.20 (s, 9H), 3.18 (s, 9H). ^{13}C NMR (126 MHz, DMSO-d_6/$CDCl_3$ (1/1 v/v)) δ 163.1, 162.8, 154.4, 153.1, 151.6, 126.1, 125.0, 122.4, 121.7, 114.1, 113.4, 97.9, 95.8, 71.8, 71.7, 70.4, 70.3, 70.2, 70.1, 69.4, 69.3, 69.2, 69.0, 68.6, 58.5, 56.9, 56.8, 56.7, 56.6. HRMS (Q-TOF) m/z: $[2M + H + Na]^{2+}$ Calcd for $C_{180}H_{253}N_{12}O_{72}Na$ 1879.3213, found 1879.3119.

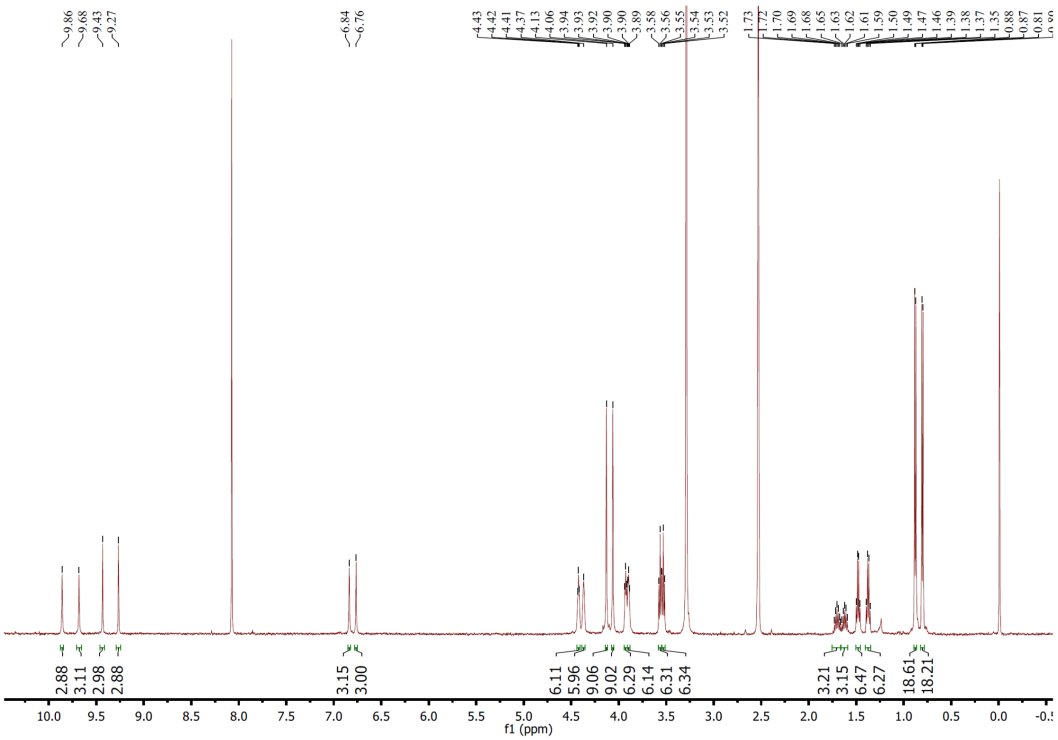

Figure S7. ^{1}H NMR (25°C, 500 MHz) spectrum of **2a** in DMSO-d_6/$CDCl_3$ (1/1, v/v).

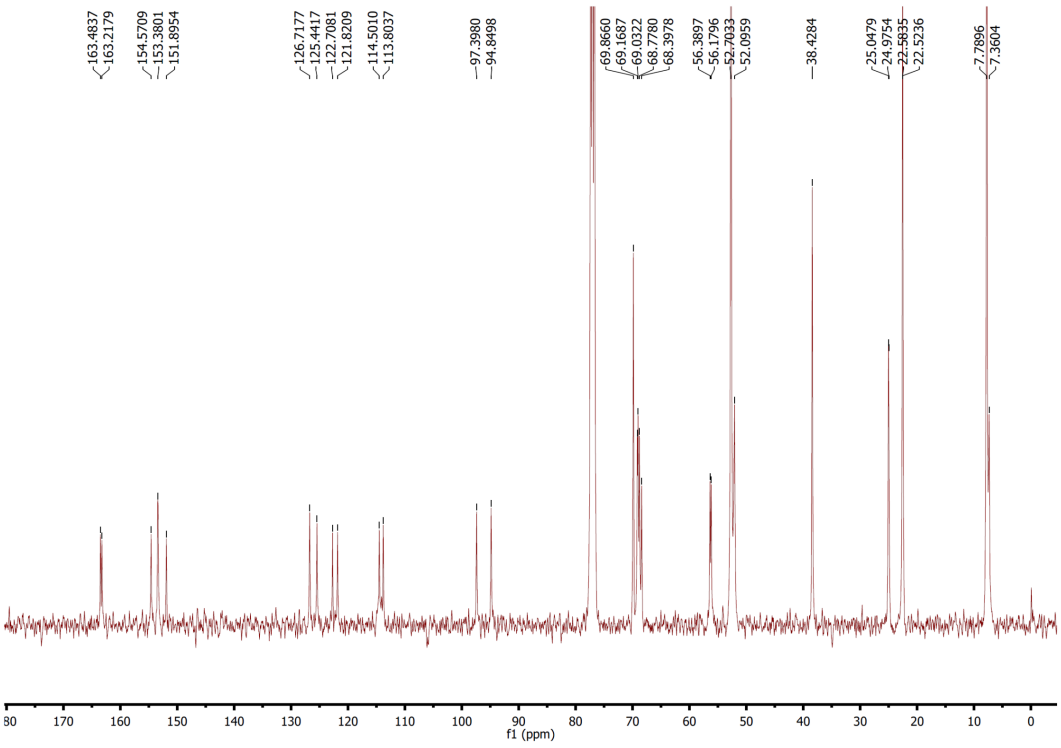

Figure S8. ^{13}C NMR (25°C, 126 MHz) spectrum of **2a** with 5 equiv. TEA-Cl in $CDCl_3$.

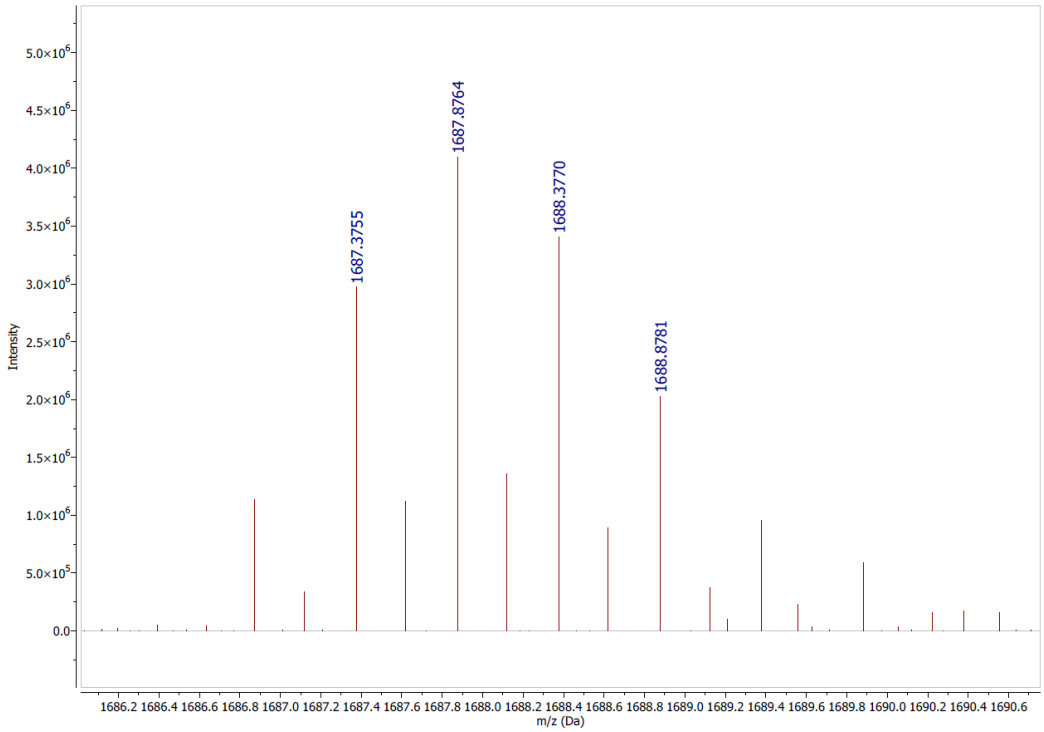

Figure S9. ESI-QTOF mass spectrum of **2a**.

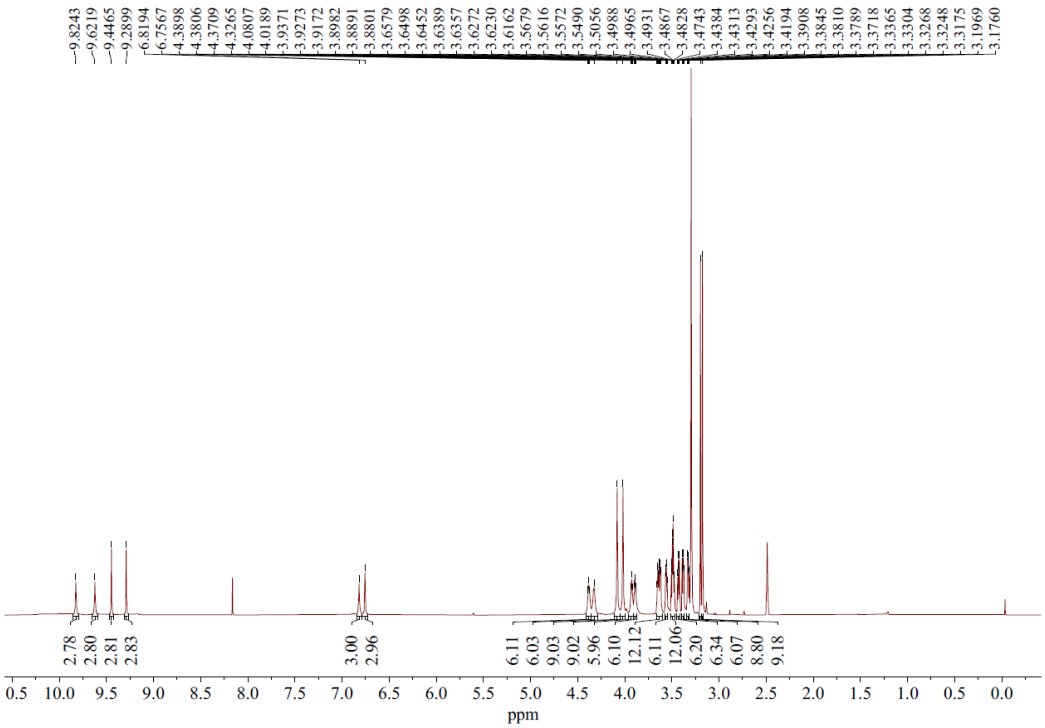

Figure S10. ^{1}H NMR (25°C, 500 MHz) spectrum of **2b** in DMSO-d_6/$CDCl_3$ (1/1, v/v).

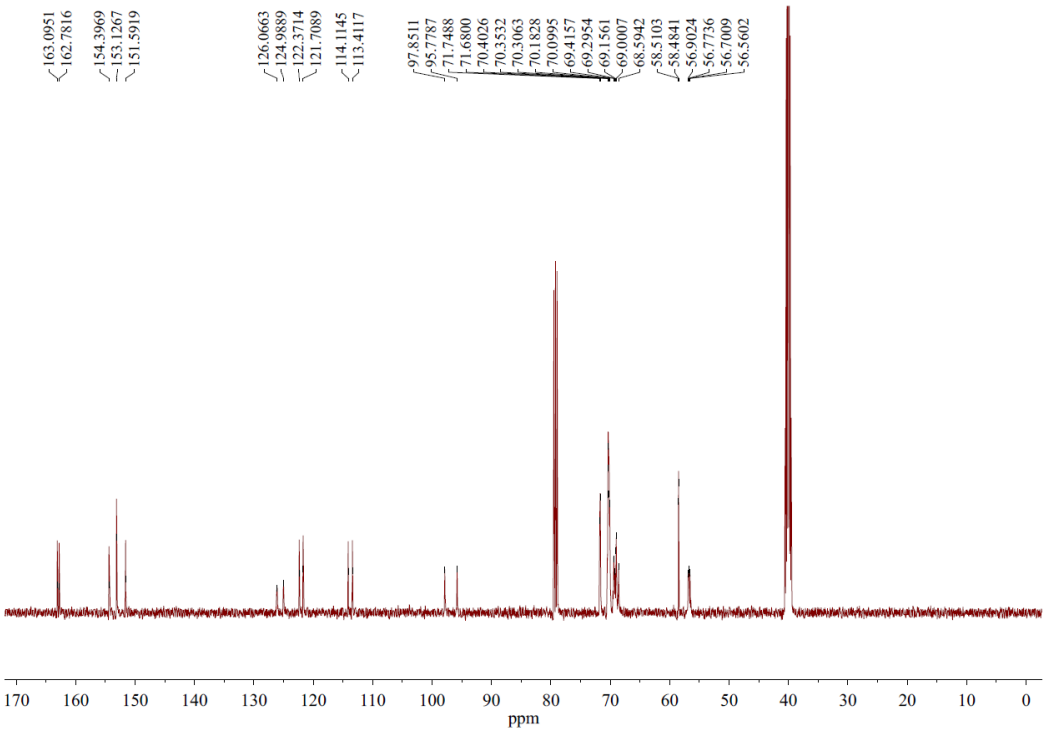

Figure S11. ^{13}C NMR (25°C, 126 MHz) spectrum of **2b** in DMSO-d_6/$CDCl_3$ (1/1, v/v).

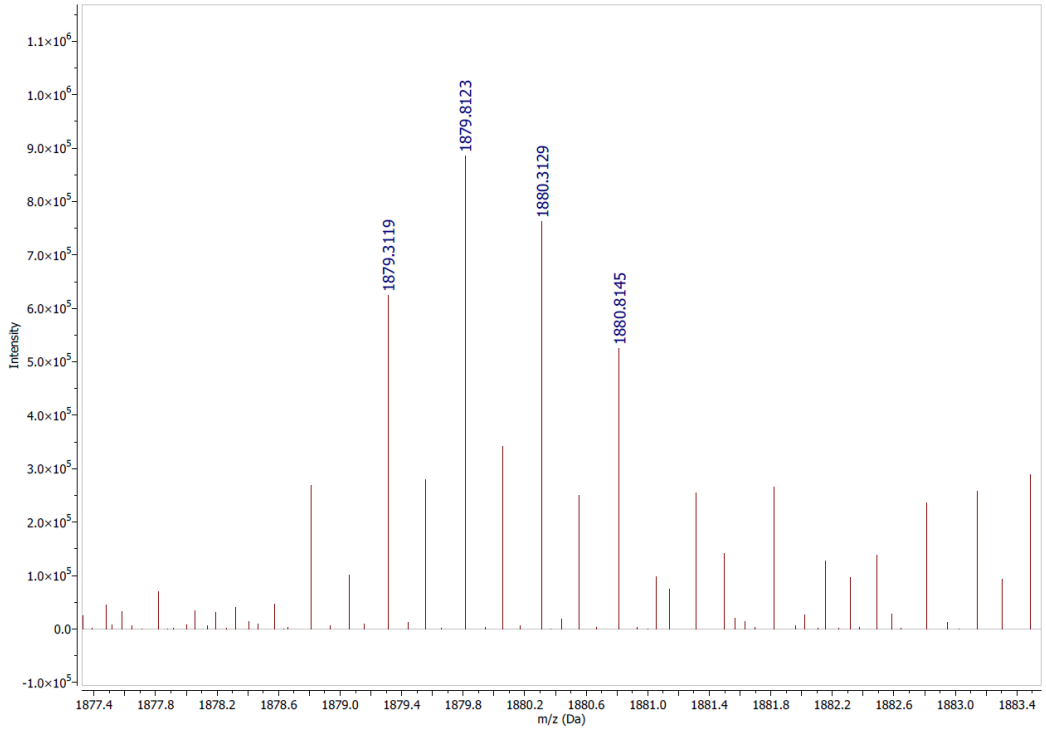

Figure S12. ESI-QTOF mass spectrum of **2b**.

IV. Computational Methods

The density functional theory calculations were performed with the ADF[3] software package. The revPBE-D3[4, 5] functional and dispersion correction, along with a TZP basis set[6], were used to geometry optimize all structures involving **2** and **G**, namely the combined 2:1 and 1:1 systems. The core electrons were frozen for the 1s electrons in oxygen, nitrogen, and carbon. Models for the host-guest interaction involving **G** with **2** were treated with a +2 overall charge on the system. The interaction energies (E_{HG}) for the 2:1 (Equation 1) and 1:1 (Equation 2) complexes were computed as follows:

$$E_{HG}\ (2{:}1) = E_{\mathbf{2{:}1}} - E_{\mathbf{G}} - 2 \times E_{\mathbf{2}} \qquad (1)$$

$$E_{HG}\ (1{:}1) = E_{\mathbf{1{:}1}} - E_{\mathbf{G}} - E_{\mathbf{2}} \qquad (2)$$

Where $E_{\mathbf{2{:}1}}$ = the computed energy of the 2:1 complex between **2** and **G**
$E_{\mathbf{1{:}1}}$ = the computed energy of the 1:1 complex between **2** and **G**
$E_{\mathbf{2}}$ = the computed energy of macrocycle **2**
$E_{\mathbf{G}}$ = the computed energy of guest **G**

An implicit solvent model (COSMO)[7] was used to model the solvent effects from the 1:1 DMSO:Chloroform solvation used in experiment. Interaction energies were calculated using structures optimized in the gas-phase and in 1:1 DMSO:chloroform solvent with the equations presented above.

Table S1. Interaction energies (kcal/mol) for the 2:1 and 1:1 systems calculated from optimizations performed in the gas-phase and in 1:1 DMSO:chloroform solvent.

2:**G**	Gas-Phase	1:1 DMSO:$CHCl_3$
Systems	E_{HG} (kcal/mol)	E_{HG} (kcal/mol)
2:1	-248.43	-100.47
1:1	-129.9	-17.14

V. Methods for X-ray Crystallography:

Single crystals of the macrocycle-paraquat complex were obtained via the liquid-liquid diffusion in an NMR tube of methanol in a dichloromethane solution of the host-guest complex (10 mg/mL).

Single crystal X-ray diffraction data for host-guest complex structures were collected with a RigakuFRX rotating anode (2.97 kW) diffractometer at the IECB X-ray facility (CNRS UMS 3033 – INSERM US001, Université de Bordeaux). CuKα radiation monochromated with high flux Osmic Varimax mirrors was used for data collection. The X-ray source is equipped with an Eiger1M detector and an AFC11 partial chi goniometer allowing omega scans. The crystals were mounted on cryoloops and flashfrozen under a nitrogen gas stream at 130(2) K. Data were processed with the CrysAlisPRO software.[8] The structure was solved with the ShelXT[9] structure solution program using Intrinsic Phasing. The Olex2 suite[10] was used for models building and structures refinement with the ShelXL[11] package running Least Squares minimization. Only non-H atoms of the backbones, guests and side chains observable in the electron density maps were refined with anisotropic displacement parameters. For backbones and observable guests or side chains H atoms were positioned geometrically and constrained depending on their environment. Those H-atoms were refined in the riding-model approximation, with Uiso(H)=1.2Ueq (CH, CH2, NH). DFIX, AFIX, and SIMU restraints were apply to model geometry of the molecules and thermal motion parameters.

Refinement of large crystal structures faces problems usually observed in macromolecular crystallography, *i.e.* large volume fractions of disordered solvent molecules radiation damage and high thermal motion for long side chains leading to weak diffraction intensities, incompleteness of the data, moderate or low resolution. Thus, it is not surprising that a number of A-level and B-level alerts were detected using IUCR's checkcif algorithm. These alerts are inherent to the data and refinement procedures and do not reflect errors.

Table S2. Crystal data and structure refinement for **2a**$_2$•**G** .

Identification code	macro_guest1_a
Empirical formula	$C_{103}H_{148}F_6N_7O_{25}P$
Formula weight	2029.25
Temperature/K	130
Crystal system	monoclinic
Space group	$P2_1/c$
a/Å	15.5642(2)
b/Å	21.6386(3)
c/Å	30.8946(3)
α/°	90
β/°	90.9030(10)
γ/°	90
Volume/Å^3	10403.6(2)
Z	4
ρ_{calc}g/cm^3	1.296
μ/mm^{-1}	0.929
F(000)	4336.0
Crystal size/mm^3	0.1 × 0.05 × 0.05
Radiation	CuKα (λ = 1.54178)
2Θ range for data collection/°	6.996 to 124.25
Reflections collected	44426
Independent reflections	14786 [R_{int} = 0.0289, R_{sigma} = 0.0366]
Data/restraints/parameters	14786/0/1301
Goodness-of-fit on F^2	1.917
Final R indexes [I>=2σ (I)]	R_1 = 0.1334, wR_2 = 0.4125
Final R indexes [all data]	R_1 = 0.1575, wR_2 = 0.4392

VI. References

1. S. Kramer, J. Langhanki, M. Krumb, T. Opatz, M. Bros and R. Zentel, *Macromol. Biosci.* 2019, **19**, 1800481.

2. Y. Zhong, B. Kauffmann, W. Xu, Z. L. Lu, Y. Ferrand, I. Huc, X. C. Zeng, R. Liu and B. Gong, *Org. Lett.* 2020, **22**, 6938.

3. G. Velde, F. F. Bickelhaupt, E. Baerends, C. Fonseca Guerra, S. van Gisbergen, J. Snijders and T. Ziegler, *J. Comput. Chem.* 2001, **22**, 931.

4. Y. Zhang and W. Yang, *Phys. Rev. Lett.* 1998, **80**, 890.

5. S. Grimme, J. Antony, S. Ehrlich and H. Krieg, *J. Chem. Phys.* 2010, **132**, 154104.

6. E. Van Lenthe and E. J. Baerends, *J. Comput. Chem*. 2003, **24**, 1142.

7. A. Klamt, *J. Phys. Chem.* 1995, **99**, 2224.

8. Rigaku Oxford Diffraction 2015. CrysAlis PRO. RigakuOxford Diffraction, Yarnton, England.

9. G. M. Sheldrick, *Acta Cryst*. 2015, **A71**, 3.

10. O. V. Dolomanov, L. J. Bourhis, R. J. Gildea, J. A. K. Howard and H. Puschmann, *J. Appl. Cryst*. 2009, **42**, 339.

11. G. M. Sheldrick, *Acta Cryst*. 2015, **C71**, 3.